SSCL-584

SSCL-584
September 1992
Distribution Category: 400

B. Moore
V. Smith
J. Reidy

Punchthrough Calculations for Neutrons Using CALOR89

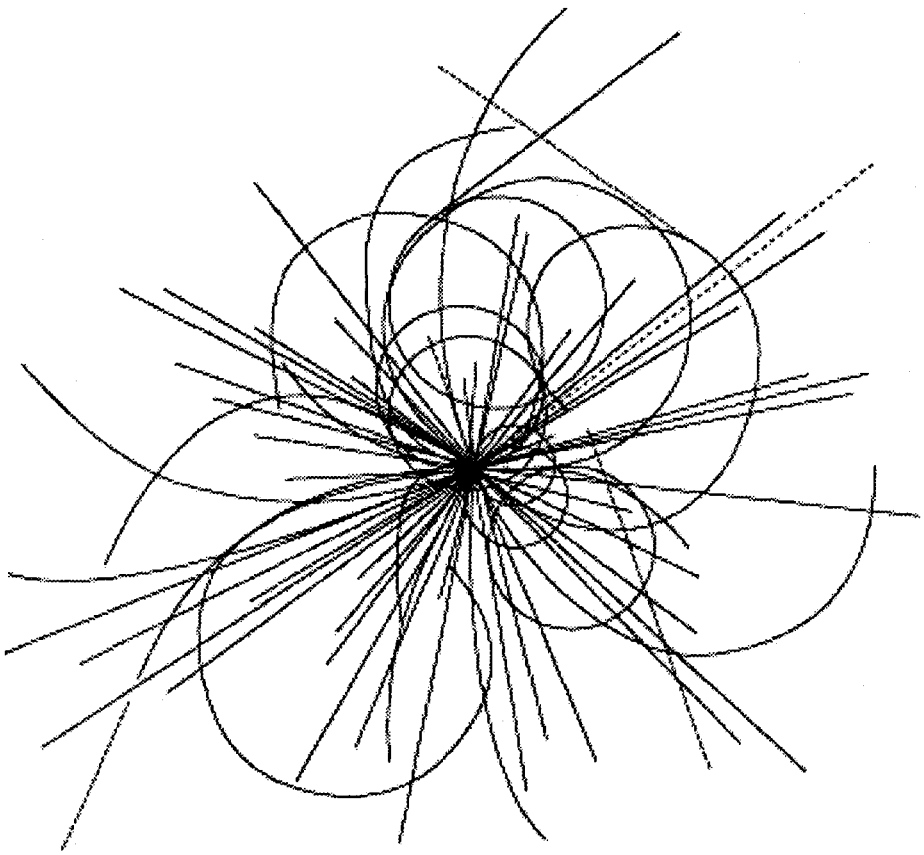

Superconducting Super Collider Laboratory

SSCL-584

Punchthrough Calculations for Neutrons Using CALOR89

B. Moore

University of Mississippi
Department of Physics, Lewis Hall
University, MS 38677

V. Smith

University of Mississippi
Department of Physics, Lewis Hall
University, MS 38677

J. Reidy

Superconducting Super Collider Laboratory*
2550 Beckleymeade Ave.
Dallas, TX 75237

September 1992

*Operated by the Universities Research Association, Inc., for the U.S. Department of Energy under Contract No. DE–AC35–89ER40486.

Punchthrough Calculations for Neutrons Using CALOR89

B. Moore, V. Smith, and J. Reidy

Abstract

Punchthrough calculations for blocks of iron, copper, depleted uranium and lead of thicknesses of 10 and 12 interaction lengths have been completed for incident negative pions of 10 GeV and 100 GeV using the CALOR89 simulation code. The most numerous particles escaping out the back of the blocks are neutrons. The simulations show that there are significantly more neutrons escaping out the back of the lead block than any of the other absorbers, despite neutron production by fission in the depleted uranium. Two effects are held to be primarily responsible for this. First, the proton and neutron shells in lead nuclei are filled, giving lead a low neutron absorption cross section relative to the other absorbers, particularly uranium. Second, the number density of lead is lower than the other absorbers, particularly copper and iron.

CONTENTS

FIGURES v
TABLES v
1.0 INTRODUCTION 1
2.0 THE CALOR89 SIMULATION PACKAGE 1
3.0 RESULTS 3
4.0 CONCLUSIONS 9
ACKNOWLEDGMENTS 11
REFERENCES 13

FIGURES

1. The Main Programs and Structure of CALOR89. 2
2. Neutron Absorption Cross Sections. 4
3. Comparison of the Number of Neutrons Escaping per Event vs. Energy for the Four Absorbers 5
4. Number of Neutrons Escaping per Event vs. Energy 6
5. Comparison of the Number of Neutrons Escaping per Square Centimeter vs. Radius, Summed Over 2500 Events for the Four Absorbers 7
6. Comparison of the Number of Neutrons Escaping per Square Centimeter vs. Radius, Summed Over 2500 Events 8

TABLES

1. Number of Neutrons per Event Escaping Out the Back of Absorber. Cutoffs on Neutrons: 500 ns, No Energy Cutoff 3
2. Number of Neutrons per Event Escaping Out the Back of Absorber. Cutoffs on Neutrons: 500 ns, 1 MeV 3
3. Number of Photons per Event Escaping Out the Back of Absorber. Cutoffs on Protons: 0.1 MeV 9

1.0 INTRODUCTION

Both the Gammas, Electrons, and Muons (GEM) and Solenoidal Detector Collaboration (SDC) groups are concerned with the possible high rates of punchthrough particles exiting the back of their hadronic calorimeters. Because of cost considerations and the space required for other components such as muon chambers and central trackers, it may be advantageous to limit the thickness of the calorimeters. One question to be addressed when considering this is how much the thickness of the calorimeters can be limited without unacceptably compromising their hermeticity. What materials should be used in view of these concerns is an important issue for GEM, which has not yet made a final decision on the absorbers, or even the technology, that will be used.

Depleted uranium has an interaction length (lambda) of 10.52 cm, but it is feared that the fission which takes place will create so many neutrons that the punchthrough rate will still be high. Simulations indicate that it is, in fact, neutrons which are of primary concern. Other materials which are under consideration are iron, copper and lead. Lead and depleted uranium have the drawbacks of high cost and the safety considerations that are associated with handling the materials. While SDC has decided on lead for the electromagnetic calorimeter and iron for the hadronic calorimeter, GEM is leaning toward using copper in the hadronic calorimeter and either copper or uranium in the electromagnetic calorimeter. It would be useful to determine how these materials compare in terms of punchthrough from incident hadrons.

We have used the CALOR89 simulation code to run punchthrough calculations for large blocks of absorbing materials. CALOR89 is generally considered to be superior to GEANT in terms of hadronic processes, and especially so for neutron transport. Blocks of 10 interaction lengths and 12 interaction lengths were considered for iron, copper, lead and depleted uranium. Showers were generated for 2500 negative pions at normal incidence upon the front face of the block with kinetic energies of 10 GeV and 100 GeV. Thus, sixteen simulations were completed, corresponding to four absorbers, two thicknesses and two energies. The blocks were 5-meters square in width in order to minimize leakage out of the side.

2.0 THE CALOR89 SIMULATION PACKAGE

The CALOR89 package has been described on numerous occasions.[1,2] The four main programs in the package are HETC88[3,4,5], SPECT, MORSE[6] or MICAP,[7] and EGS4.[8] A flow diagram of UNIX Version 3[9] of CALOR89 is shown in Figure 1. This was built at the University of Mississippi starting from an IBM version of the package that was created at Oak Ridge. Some of the programs had been modified by Tom Handler of the University of Tennessee.

HETC88 is the principal program. It transports all the hadronic particles except neutrons which are below 20 MeV. Neutrons which are below 20 MeV are transported by MORSE. Any electromagnetic particles which are generated are transported by EGS4. There are three models which are used in HETC88. An intermediate-energy intranuclear-cascade evaporation model is used at energies below 3 GeV. Above 3 GeV, a scaling model is used. Above the energy given by ESKALE, a parameter set by the user, the FLUKA87[10] code of J. Ranft, *et al.* is implemented instead; a code which uses a multi-chain fragmentation model. The exact value that should be used for ESKALE is not yet clear, but it is generally thought to be between 5 GeV and 20 GeV. We set ESKALE at 15 GeV, so the FLUKA model was not used at all for the runs with the 10 GeV incident pions. Also included are elastic and inelastic hydrogen collisions, elastic neutron-nucleus collisions ($E < 100$ MeV), decay of particles, and energy loss of charged particles due to ionization collisions. Everything that happens is written out to a history file: collisions, boundary crossings, creation of particles, escapes, *etc.*

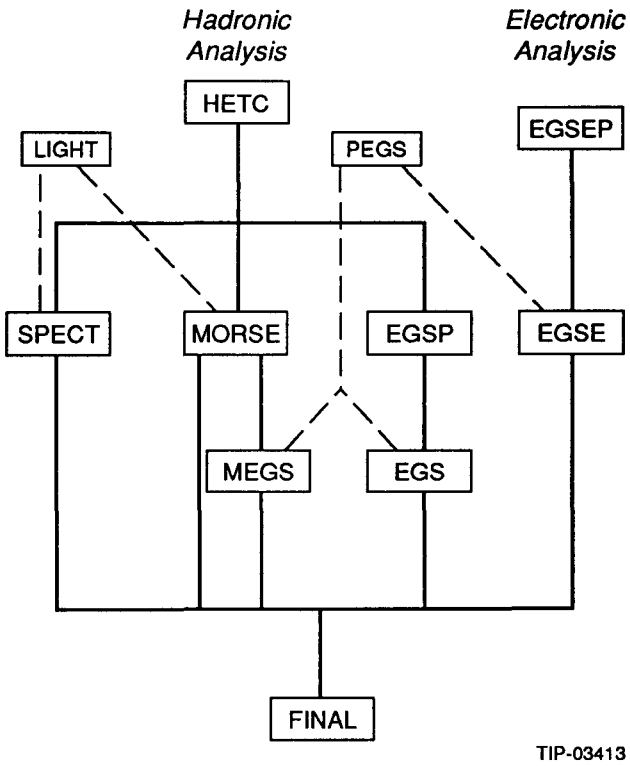

Figure 1. The Main Programs and Structure of CALOR89.

SPECT89 analyzes the results of the hadronic transport in HETC. For the purposes of this calculation, it was used merely to record the escapes out the back of the blocks that had already been written out to the HETC history file.

MORSE transports all neutrons with kinetic energy below 20 MeV. Neutrons from HETC which reach or are produced below this cutoff are not transported by HETC, but are written out to the HETC history file to be picked up and transported by MORSE. Photons may be generated in MORSE through neutron capture, fission, and inelastic collisions. These photons are then written out to a MORSE history file so that they can be picked up and transported by EGS4. MORSE has time dependence built into the code, and a time cutoff of 500 ns was used. Neutrons older than 500 ns can escape from the absorber, but will have very low energy, and direct collisions of these neutrons in muon chambers can only produce small signals. However, gamma rays emitted from the capture of such low energy neutrons may produce significant backgrounds.

EGS4 is used to transport the electromagnetic component of the hadronic shower in two phases. The HETC history file is read by EGSPREP, which then writes out a file that is readable by EGS and that contains only information on the electromagnetic particles generated. EGS is then run to transport the electromagnetic particles produced in HETC. As mentioned in the preceding paragraph, MORSE writes out a list of photons generated into a MORSE history file, which is readable by a program called MOREGS. MOREGS is almost identical to EGS, but includes code to incorporate the time information which is passed on from MORSE.

Certain parameters associated with escaping particles, such as the kinetic energy, particle type, point of exit, and direction of propagation, were written out by SPECT, MORSE, EGS, and MOREGS and subsequently read by a final analysis program. We were primarily concerned with the neutron punchthrough, so the outputs of SPECT and MORSE were of greatest interest to us, although it is also interesting to make note of the photon punchthrough.

3.0 RESULTS

Table 1 gives the results on the number of neutrons which escaped out the back of the block for the various absorbers, depths and incident pion energies. Results are also given in Table 2 with a 1 MeV cutoff applied in the final analysis program.

TABLE 1. NUMBER OF NEUTRONS PER EVENT ESCAPING OUT THE BACK OF ABSORBER. CUTOFFS ON NEUTRONS: 500 ns, NO ENERGY CUTOFF.

10 GeV Pi^-	10 Lambda	12 Lambda
Copper	0.81 ± 0.06	0.15 ± 0.02
Iron	0.94 ± 0.06	0.24 ± 0.03
Uranium	2.3 ± 0.2	0.8 ± 0.1
Lead	4.8 ± 0.2	1.22 ± 0.08
100 GeV Pi^-		
Copper	15.2 ± 0.5	5.0 ± 0.3
Iron	17.9 ± 0.5	6.4 ± 0.3
Uranium	50.0 ± 2.0	16. ± 1.0
Lead	74.0 ± 2.0	25. ± 1.0

TABLE 2. NUMBER OF NEUTRONS PER EVENT ESCAPING OUT THE BACK OF ABSORBER. CUTOFFS ON NEUTRONS: 500 ns, 1 MeV.

10 GeV Pi^-	10 Lambda	12 Lambda
Copper	0.23 ± 0.02	0.041 ± 0.007
Iron	0.19 ± 0.02	0.040 ± 0.006
Uranium	0.36 ± 0.05	0.14 ± 0.03
Lead	0.67 ± 0.05	0.14 ± 0.02
100 GeV Pi^-		
Copper	4.2 ± 0.2	1.38 ± 0.08
Iron	4.0 ± 0.2	1.38 ± 0.08
Uranium	8.5 ± 0.4	2.8 ± 0.2
Lead	13.1 ± 0.6	4.1 ± 0.3

A rather surprising result is immediately apparent. That is there are 50% to 100% more neutrons escaping from the lead than the depleted uranium, depending on the energy of the incident pion and thickness of the absorber. This is true despite the fact that fission processes should be producing neutrons in much larger numbers in the uranium than neutrons could be produced in the lead. We believe a large part of the reason for this is that lead is a "magic" element. With 82 protons, the proton shell in the lead nucleus is filled.[11] This would tend to make lead somewhat resistant to absorbing neutrons—at least via reactions that would change the number of protons in the nucleus. Further, Pb-208, which constitutes 52.3% of naturally occurring lead,[12] is doubly magic because the neutron shell, containing 126 neutrons, is also filled. Half of lead nuclei, therefore, will be extremely resistant to interacting with neutrons near or below the nuclear binding energy because they will tend to keep just exactly the same number of both neutrons and protons.

This is reflected in the Figure 2 graphs, which show the neutron absorption cross section for copper, iron, U-238, and lead. These cross sections were obtained from MORSE by setting a flag which causes the program to print out the cross sections used. These cross sections are from ENDFB/V. The resistance of the lead to reacting with neutrons is demonstrated by the fact that it has a very low neutron absorption cross section. Only iron is comparable in the range from about 30 keV to 2 MeV. Specifically, the cross section for lead is roughly 15 times smaller than that of iron and 35 times smaller than copper. These numbers were obtained simply by averaging the cross sections over each of the 105 energy groups the neutrons are divided into by MORSE. The absorption cross section for uranium is quite high, running about 1700 times greater than lead. This high cross section for the uranium no doubt plays a large role in countering fission effects.

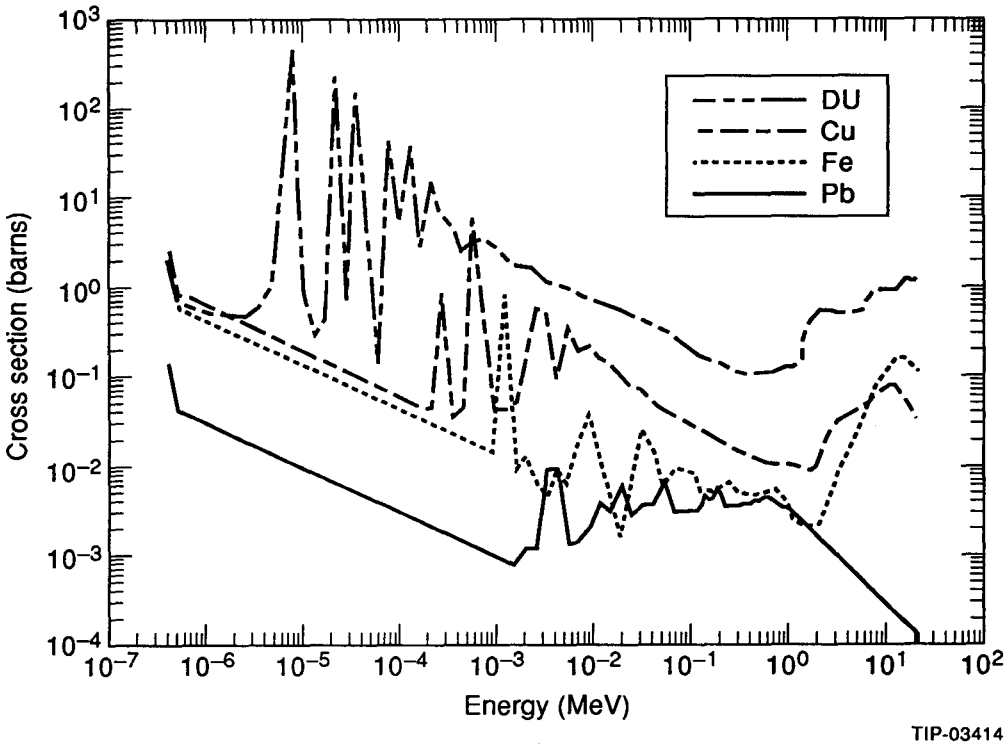

Figure 2. Neutron Absorption Cross Sections.

Also of some importance, if a little less interesting, is the fact that lead nuclei are less abundant than those of the other absorbers. The number density of lead is 3.3×10^{22} nuclei per cubic centimeter, while the number density for depleted uranium is $4.79 \times 10^{22}/cm^3$, and for both iron and copper it is $8.49 \times 10^{22}/cm^3$. Quite simply, there are considerably fewer nuclei for neutrons to interact with in lead than in iron or copper, and somewhat fewer than in uranium.

We believe that these two effects are chiefly responsible for making lead relatively transparent to neutrons compared with copper, iron and depleted uranium.

The importance of the neutron absorption cross section is indicated by the neutrons escaping from iron and copper as shown in Table 1 for all neutrons and in Table 2 for neutrons with at least 1 MeV kinetic energy. While slightly fewer neutrons tend to punch through the copper than the iron overall, among neutrons which escape with at least 1 MeV kinetic energy, the copper is no better than the iron and may actually be slightly worse. From Figure 2, we see that the neutron absorption cross section for iron is greater than for copper from about 6 MeV up to 20 MeV, and on average it is higher by a factor of about 1.5 above 1 MeV. Though other factors may have an influence, it is clear that the neutron absorption cross section is significant. This makes for a nice comparison because the number densities of copper and iron nuclei are almost identical.

Figures 3 and 4 show the energy distribution for each of the four absorbers for the 100 GeV pion incident upon 10 interaction lengths. The number of punchthrough neutrons per event is plotted versus energy. One can see that a greater proportion of the neutrons in lead are above 0.5 MeV than in the other absorbers, particularly in the range 0.5–2.0 MeV.

Figures 5 and 6 show the density of escaping neutrons for the same runs as a function of distance from the center of the back face, which is where the pion would have come out had it passed directly through the block without interacting or decaying. The vertical axis is the number of neutrons per square centimeter. These graphs contain data summed over all 2500 events, so one would divide the numbers by 2500 to get the neutrons-per-square-centimeter-per-event. Notice that the uranium shower is much more focused than the other showers, which one may expect considering it has the highest neutron absorption cross section. The lead, on the other hand, has the lowest such cross section, and one sees that the lead shower is more spread out, again, as one would expect.

In Table 3, the number of photons escaping out the back per event is shown for each of the runs. In terms of photon punchthrough, the lead is the best absorber at all energies and uranium generally appears to be better than the copper and iron. This is to be expected. The apparent exception at twelve lambda for the 10 GeV iron may not be statistically significant. The radiation lengths are 0.56 and 0.32 cm, respectively, for lead and uranium, while the radiation lengths for iron and copper are 1.76 and 1.43 cm.

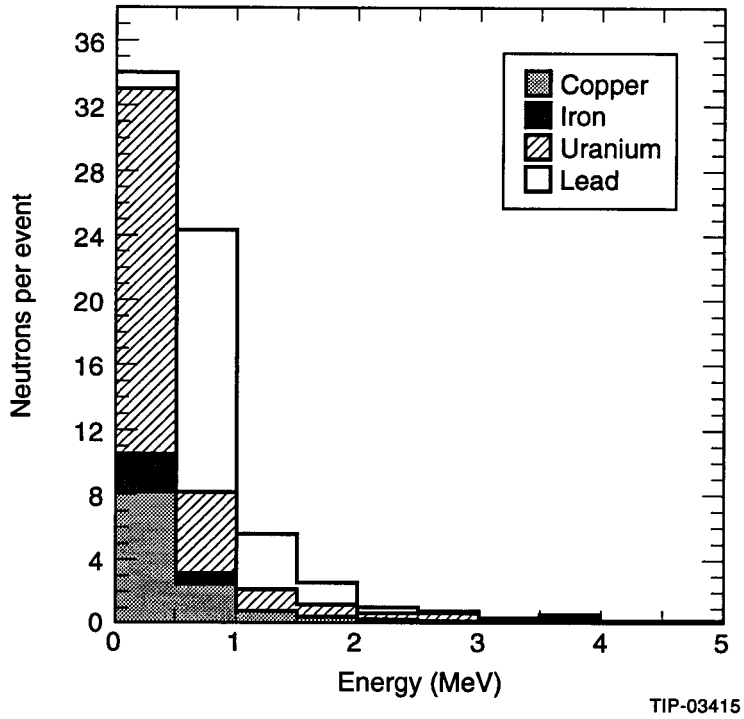

Figure 3. Comparison of the Number of Neutrons Escaping per Event vs. Energy for the Four Absorbers.

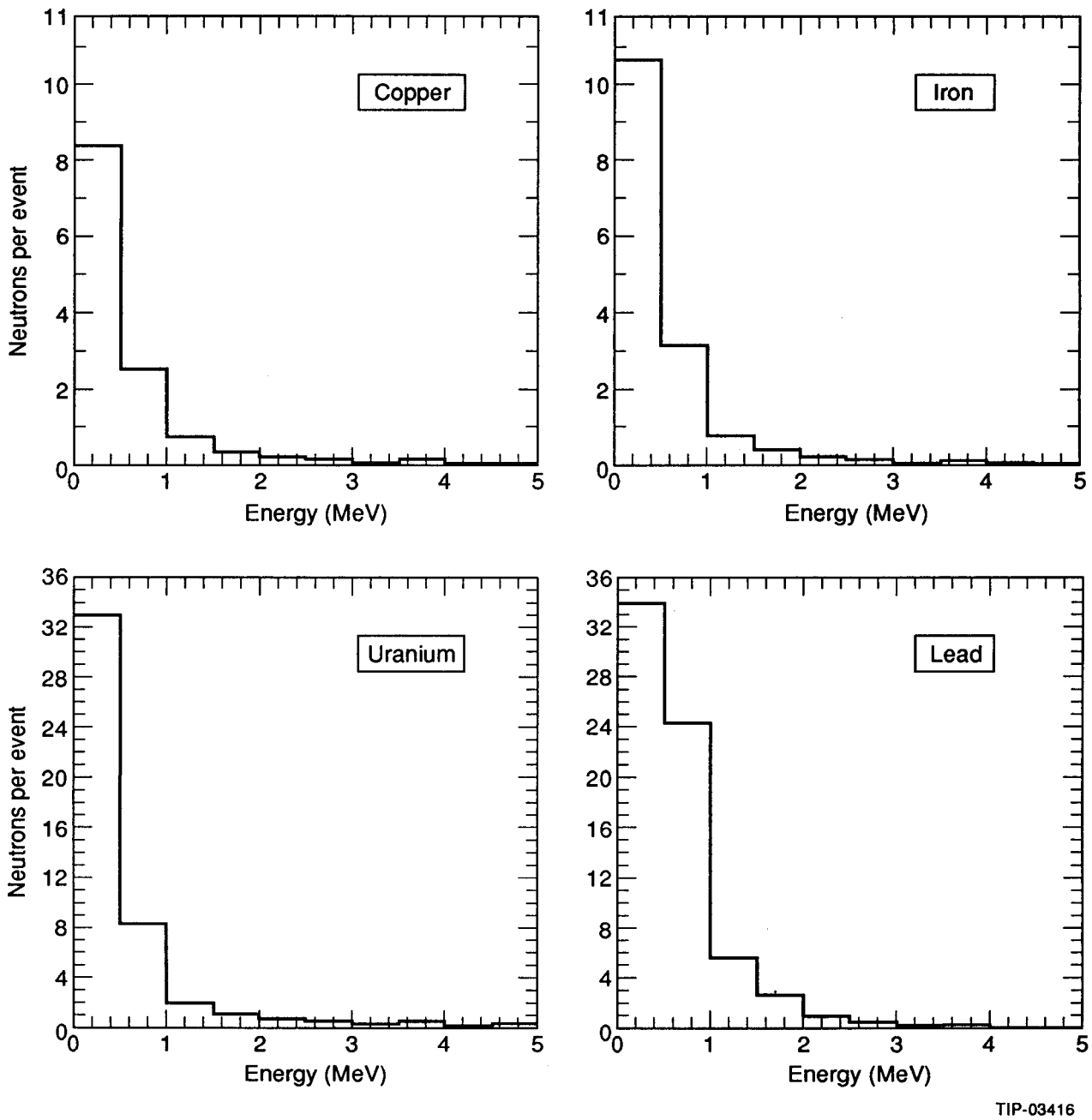

Figure 4. Number of Neutrons Escaping per Event vs Energy.

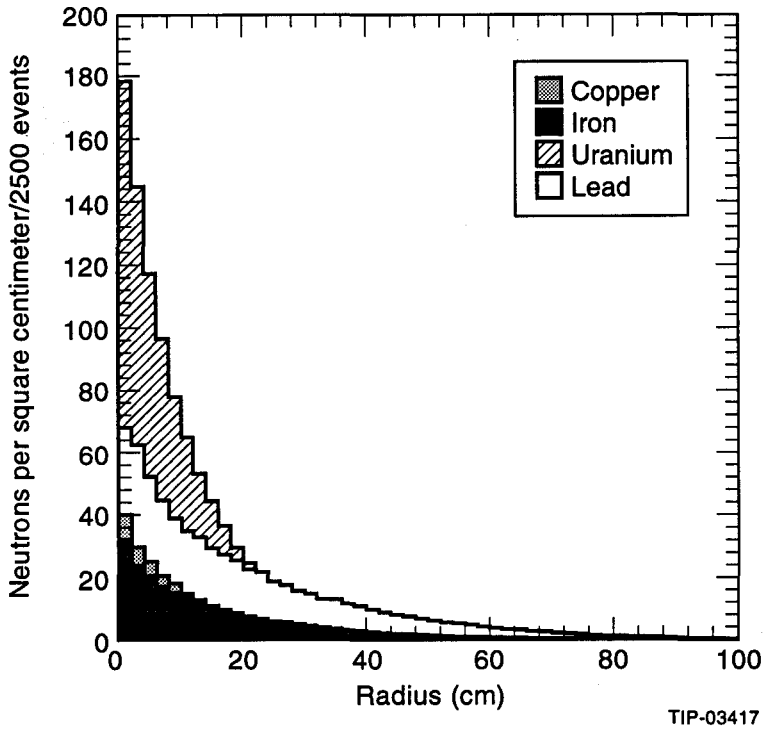

Figure 5. Comparison of the Number of Neutrons Escaping per Square Centimeter vs. Radius, Summed over 2500 Events for the Four Absorbers.

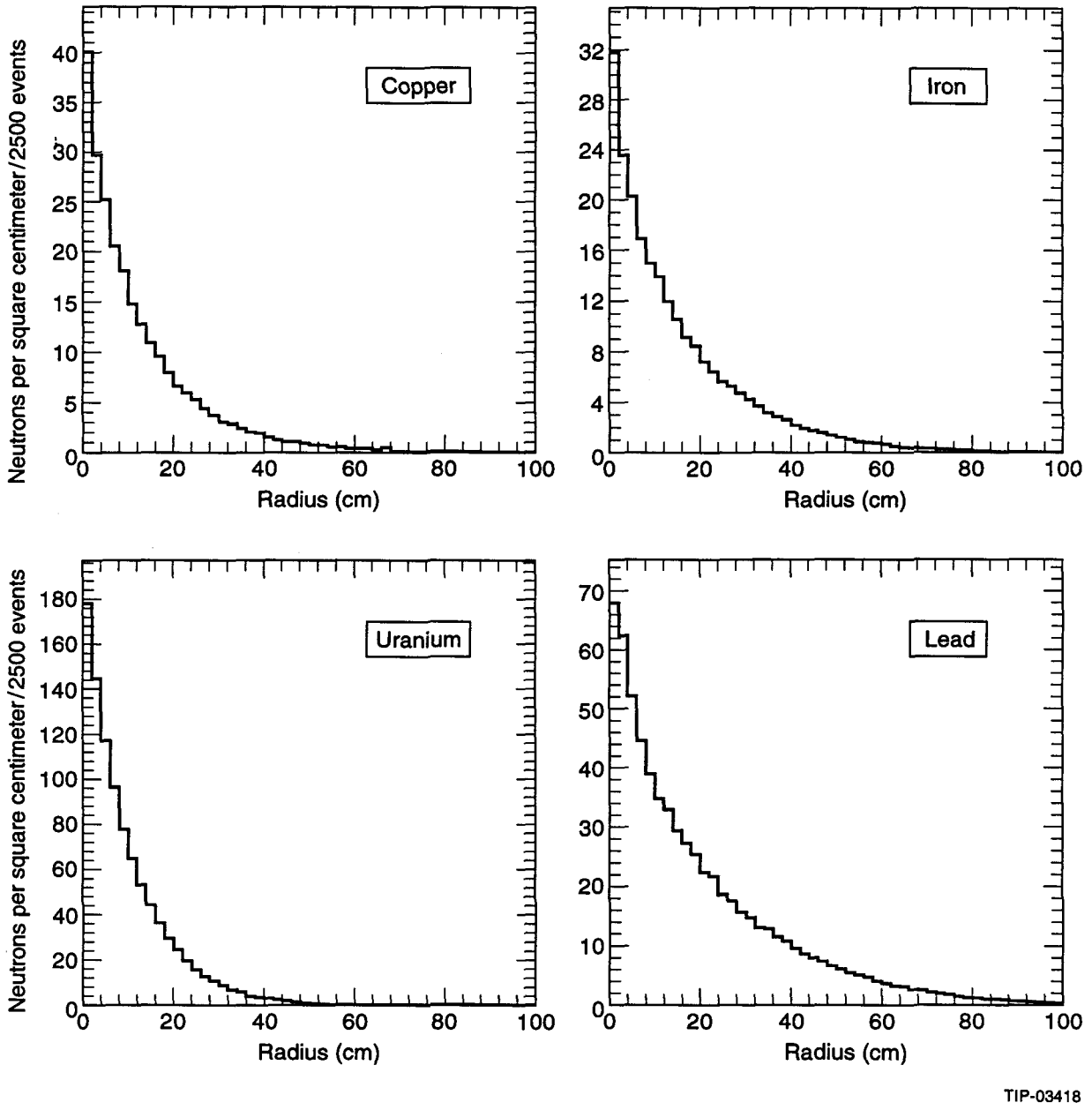

Figure 6. Comparison of the Number of Neutrons Escaping per Square Centimeter vs. Radius, Summed Over 2500 Events.

TABLE 3. NUMBER OF PHOTONS PER EVENT ESCAPING OUT THE BACK OF ABSORBER. CUTOFFS ON PHOTONS: 0.1 MeV.

10 GeV Pi^-	10 Lambda	12 Lambda
Copper	0.07 ± 0.02	0.020 ± 0.009
Iron	0.030 ± 0.006	0.004 ± 0.002
Uranium	0.035 ± 0.006	0.02 ± 0.01
Lead	0.010 ± 0.007	0.003 ± 0.002
100 GeV Pi^-		
Copper	7.0 ± 1.0	2.2 ± 0.7
Iron	9.0 ± 2.0	2.2 ± 0.6
Uranium	1.7 ± 0.3	0.5 ± 0.1
Lead	1.3 ± 0.4	0.16 ± 0.06

4.0 CONCLUSIONS

Our punchthrough calculations with CALOR89 using an incident pion of 10 GeV and 100 GeV upon blocks of absorber 10 and 12 interaction lengths thick indicate that copper and iron do a better job of preventing neutron punchthrough than uranium and lead, but are worse in terms of photon punchthrough. The lead has the highest rate of neutron punchthrough in part because the number density of lead nuclei is smaller, but primarily because of the very small neutron absorption cross section. Uranium has the next highest rate of neutron punchthrough despite having a very high neutron absorption cross section because fission produces neutrons in large quantities.

ACKNOWLEDGMENTS

Thanks go to Roger McNeill of Louisiana State University, who has devoted much time and effort to punchthrough considerations, for discussions concerning the neutron and photon punchthrough and for first suggesting we try some punchthrough calculations with CALOR. We would like to express our appreciation to Tony Gabriel of Oak Ridge National Laboratory, Konstantin Shmakov of the University of Tennessee, and to Lee Bolen and Lucien Cremaldi of the University of Mississippi for helpful discussions. Financial support for this research was provided by the Texas National Research Laboratory Commission and by the U.S. Department of Energy through grant number DE-FG05–91ER40622.

REFERENCES

1. T. A. Gabriel, J. E. Brau, B. L. Bishop, *IEEE Trans. Nucl. Sci.,* **36** (1989), p. 14.
2. T. A. Gabriel, *et al.,* "CALOR89: Calorimetry Analysis and Benchmarking," *Proceedings of the First International Conference on Calorimetry in High Energy Physics,* eds. Anderson, *et al.*, World Scientific, Singapore (1991).
3. T. A. Gabriel, "The High Energy Transport Code HETC," Oak Ridge National Laboratory, ORNL/TM-9727 (1985).
4. T. A. Gabriel, *et al.,* "CALOR87: HETC87, MICAP, EGS4, and SPECT: A Code System for Analyzing Detectors for Use in High Energy Physics Experiments," *Proceedings of the Workshop on Detector Simulations for the SSC,* Argonne National Laboratory (1987).
5. R. G. Alsmiller, Jr., F. S. Alsmiller, and O. W. Hermann, *Nucl. Inst. & Meth.,* **A295** (1990), p. 337.
6. M. B. Emmett, "The MORSE Monte Carlo Radiation Transport Code System," Oak Ridge National Laboratory, ORNL-4972 (1975), ORNL-4972/Rl (1983), ORNL-4972/R2 (1984).
7. J. O. Johnson and T. A. Gabriel, *A User's Guide to MICAP: A Monte Carlo Ionization Chamber Analysis Package,* Oak Ridge National Laboratory, ORNL/TM-10196 (1987).
8. W. R. Nelson, *et al.,* Stanford Linear Accelerator Center, SLAC-265, (1985).
9. B. R. Moore, *User's Guide to CALOR89–U3G on PDSF,* SDC-92–246 (1992).
10. P. A. Aarnio, *et al.*, CERN TIS Divisional Report, TIS-RP/106–Rev (1984).
11. A. Klimov, *Nuclear Physics and Nuclear Reactors,* Mir Publishers, Moscow (1975).
12. M. R. Wehr, J. A. Richards, Jr., and T. W. Adair, *Physics of the Atom,* Addison-Wesley, Reading, MA (1978).